# Novel Methods for CVD of $Ge_4C$ and $(Ge_4C)_xSi_y$ Diamond-like Semiconductor Heterostructures: Synthetic Pathways and Structures of Trigermyl-$(GeH_3)_3CH$ and Tetragermyl-$(GeH_3)_4C$ Methanes

**J. Kouvetakis,*,[†] Arne Haaland,*,[‡] Dmitry J. Shorokhov,[‡] Hans Vidar Volden,[‡]
Georgii V. Girichev,[§] Vasili I. Sokolov,[§] and Phillip Matsunaga[†]**

*Contribution from the Department of Chemistry, Arizona State University, Tempe, Arizona 85287, Department of Chemistry, University of Oslo, Box 1033 Blindern, N-0315 Oslo, Norway, and Department of Physics, State Academy of Chemical Technology, 153460 Ivanovo, Russia*

*Received March 24, 1998*

**Abstract:** $GeX_2\cdot$dioxane (X = Cl, Br) complexes insert completely into $CBr_4$ to afford the sterically crowded cluster compounds $(BrCl_2Ge)_4C$ (**1**) and $(Br_3Ge)_4C$ (**2**) in 80% and 95% yields, respectively. These display physical, spectroscopic, and structural properties that are indicative of highly symmetric molecules with a remarkably strained carbon center. Compounds **1** and **2** react with $LiAlH_4$ to produce the hydrides $(H_3Ge)_3CH$ (**3**) and $(H_3Ge)_4C$ (**4**) which are readily identified and characterized by spectroscopic methods and gas-phase electron diffraction. Compound **3** is also conveniently prepared from the $LiAlH_4$ reduction of $(GeBr_3)_3CH$ (**5**) which in turn is obtained by insertion of $GeBr_2\cdot$dioxane into the C−Br bonds of bromoform. Refinement of the diffraction data for **3** confirmed a model of $C_3$ symmetry, with local $C_{3v}$ symmetry of the $GeH_3$ groups, and gave a Ge−C bond length of 1.96 Å. The structure refinement of **4** was based on a model of $T$ symmetry and displayed a rather normal Ge−C bond distance of 1.97 Å, which is substantially shorter than that (2.049 Å) of the strained $(Br_3Ge)_4C$ (**2**) compound. Density functional calculations closely reproduced the observed molecular structures for **3** and **4**. The thermal dehydrogenation of **4** on (100) Si surfaces at 500 °C resulted in the growth of a diamond-structured material with an approximate composition of $Ge_4C$. Reactions of **4** with $(SiH_3)_2$ on Si yielded heteroepitaxial growth of metastable, monocrystalline $(Ge_4C)_xSi_y$ alloy semiconductors that are intended to have band gaps wider than those of pure Si and $Si_{1-x}Ge_x$ alloys and strained superlattices. The covalent cluster species described here not only are of intrinsic molecular interest but also provide a unique route to a new class of semiconductor materials and form a model for local carbon sites in Ge−C crystals and related electronic materials based on the diamond structure.

## Introduction

The successful creation of a band gap-engineered heterojunction bipolar transistor (HBT) from $Si_{1-x}Ge_x$ alloys has led to the tremendous interest in the synthesis of metastable, $Si_{1-x-y}Ge_xC_y$ random alloys on silicon.[1] The presence of carbon in the lattice is intended to reduce the inherent lattice mismatch between SiGe and the Si substrate with the small size of carbon compensating for the larger germanium. Lattice matching reduces strain defects and promotes epitaxial film growth which is necessary for effective device performance. $Ge_{1-x}C_x$ alloys with suitable carbon concentrations should also match dimensionally the lattice of Si (the lattice parameter of Si is intermediate to that of pure Ge and diamond) and thus allow growth of strain-free heteroepitaxial layers on single-crystal Si. This simpler binary system also offers the potential for band gap engineering, and in theory band gaps greater than those of Ge, Si−Ge, or even Si are expected with increasing carbon concentration. Wide band gap $Ge_{1-x}C_x$ superlattices are likely to have important technological applications in high-speed heterojunction bipolar transistors and optoelectronics.[2−4]

Very recently, we demonstrated that reactions of $(SiH_3)_4C$ (a C−H free C and Si precursor molecule) with $GeH_4$ and $SiH_4$ on (100) Si form metastable, diamond-structured $Si_{1-x-y}Ge_xC_y$ random alloys that contain 4−6 atom % carbon, the highest carbon content incorporated in crystalline Si−Ge−C.[5,6] In these systems, generally accepted as ideal solutions, we observed the formation of an unusual $(Si_2Ge)C_x$ ordered structure of $P\bar{3}m1$ symmetry formed by Ge−Si−Si ordering along the diamond (111) direction. A small concentration of carbon that is incorporated into the Si−Si bilayer of the material as $Si_4C$ tetrahedra is the key to the formation of this ordered phase.[7]

---

[†] Arizona State University.

[‡] University of Oslo.

[§] State Academy of Chemical Technology.

(1) Iyer, S. S.; Patton, G. L.; Stork, J. M.; Meyerson, B. S.; Harame, D. L. *IEEE Trans. Electron. Dev.* **1989**, *36*, 2043.

(2) (a) Osten, H. J.; Bugiel, E.; Zaumseil, P. *J. Cryst. Growth* **1994**, *142*, 322−326. (b) Osten, H. J.; Klatt, J. *Appl. Phys. Lett.* **1994**, *65*, 2960−2962. (c) Krishnamurthy, M.; Drucker, J. S.; Challa, A. *J. Appl. Phys.* **1995**, *78*, 7070−7073. (d) Kolodzey, J.; O'Neil, P. A.; Zhang, S.; Orner, B. A.; Roe, K.; Unruh, K. M.; Swann, C. P.; Waite, M. M.; Ismat Shah, S. *Appl. Phys. Lett.* **1995**, *67*, 1865.

(3) Todd. M.; Kouvetakis, J.; Smith, D. J. *Appl. Phys. Lett.* **1996**, 2407. Todd, M.; McMurran, J.; Kouvetakis, J.; Smith, D. J. *Chem. Mater.* **1996**, *8*, 2491.

(4) Soref, R. F. *J. Appl. Phys.* **1991**, *70*, 2470.

(5) Kouvetakis, J.; Todd, M.; Chandrasekhar, D.; Smith, D. J. *Appl. Phys. Lett.* **1994**, *65*, 2960.

(6) Todd, M.; Matsunaga P.; Kouvetakis, J.; Chandrasekhar, D.; Smith, D. J. *Appl. Phys. Lett.* **1995**, *67*, 1247.

(7) Kouvetakis, J.; Nesting, D. C.; O'Keeffe, M.; Smith, D. J. *Chem. Mater.* **1998**, *10*, 1396.

S0002-7863(98)01003-8 CCC: $15.00

Furthermore, the dehydrogenation of $C(SiH_3)_4$ at 500 °C on Si followed by solid-phase epitaxy at 800 °C produced a completely novel compound semiconductor of composition $Si_4C$.[8] This monocrystalline phase consists of $Si_4C$ tetrahedra linked together in a three-dimensional diamond-like network and was theoretically predicted earlier by Rucker et al.[9]

The propensity of the $(SiH_3)_4C$ compound to maintain the $Si_4C$ composition and structure in the solid state suggests that the analogous $(GeH_3)_4C$ molecule may be a source of $Ge_4C$ tetrahedral units which are considered ideal building blocks for the synthesis of new materials such as random alloys and ordered phases in the Ge−C and Si−Ge−C systems. The lack of strong C−H bonds and the presence of the relatively weak Ge−H bonds in this precursor will favor lower deposition temperatures thus leading to new metastable structures and compositions. We anticipate that lower growth temperatures should permit higher carbon incorporation (C > 5 atom %) which is considered necessary to affect the lattice parameter and influence the band gap in these systems. Another advantage is the absence of Si−C bonds, which at high processing temperatures would favor SiC precipitation and cause phase segregation in these thermodynamically unstable Si−Ge−C heterostructures. Finally, the epitaxial formation of the metastable and potentially ordered $Ge_4C$ phase, which may be obtained by the thermal dehydrogenation reaction of $(GeH_3)_4C$ on Si, is of interest.

In a brief Communication, we recently reported synthetic pathways to the extremely crowded (trihalogermyl) methanes $(GeBr_3)_4C$ (**1**) and $(GeBrCl_2)_4C$ (**2**) and their reduction to produce $(GeH_3)_3CH$ (**3**) and $(GeH_3)_4C$ (**4**) in very low yields (1%).[10] Such yields were suitable for preliminary characterization of these compounds but certainly insufficient for exploring their application as viable precursors to Si−Ge−C semiconductor materials by chemical vapor deposition (CVD). Continuing efforts have focused on development of a better preparative method and also a complete characterization of this new family of germyl methanes. In this paper, we report substantial improvements on the synthesis of $(GeH_3)_4C$ and $(GeH_3)_3CH$ (which is also obtained by reduction of $(GeBr_3)_3CH$ (**5**)) and provide a full description of the synthesis, characterization, and properties of compounds **1**−**5**. We also describe the molecular structures for $(GeH_3)_4C$ and $(GeH_3)_3CH$ as obtained by gas-phase electron diffraction (GED). The structural characterization of **4** was undertaken to completely characterize the compound and, more importantly, to determine the Ge−C bonding interactions in the $Ge_4C$ tetrahedral core of $(GeH_3)_4C$. The structure of $(GeH_3)_3CH$ was determined to confirm the identity of the compound and to compare bond lengths between the seemingly crowded $Ge_4C$ core of **4** and the less crowded $Ge_3CH$ core of **3**. The bonding parameters described in this study, particularly those of the tetrahedral compounds **2** and **4**, are important with regard to structural characterization and theoretical modeling of crystalline Ge−C tetrahedral semiconductor systems.[11] Finally preliminary results on the utilization of **3** and **4** to grow new Ge−C and Si−Ge−C epitaxial materials are presented.

## Results and Discussion

**Synthesis and Characterization of $(H_3Ge)_3CH$ (3) and $(H_3Ge)_4C$ (4).** The germylene complexes, $GeX_2$·dioxane (X = Cl, Br), undergo complete insertion into the C−Br bonds of $CBr_4$ to give the tetrakis(trihalogermyl)methane compounds, $(BrCl_2Ge)_4C$ (**1**) and $(Br_3Ge)_4C$ (**2**), in 80% and 94% yields, respectively (eq 1).[10] Dihalogermylenes and their base adducts have been shown previously to be reactive toward C−X and C−C multiple bonds. However, this is the first example of germylene insertion leading to complete substitution at a single C center.[12]

$$4GeX_2\cdot\text{dioxane} + CBr_4 \rightarrow \underset{\mathbf{1,\,2}}{(X_2BrGe)_4C} + 4\text{dioxane} \quad (X = Cl, Br) \quad (1)$$

Compounds **1** and **2** are crystalline, air-stable, high-melting solids that behave similarly to other highly symmetric compounds containing a tetrahedral core of group IVA elements.[13] The reduction of **2** with $LiAlH_4$ leads to the target compound $(H_3Ge)_4C$ (**4**) which is isolated in 20% yield. A substantial quantity (18% yield) of $(H_3Ge)_3CH$ (**3**), the tris(germyl) analogue, is also obtained as a byproduct from the reduction of **2** (eq 2).

$$\underset{\mathbf{2}}{(Br_3Ge)_4C} \xrightarrow{LiAlH_4} \underset{\mathbf{3}}{(H_3Ge)_3CH} + \underset{\mathbf{4}}{(GeH_3)_4C} \qquad (2)$$

The reduction takes place in a very high boiling solvent, 2,6,10,15,19,23-hexamethyl-2,6,10,14,18,22-tetracosahexaene ($C_{30}H_{50}$ squalene), in a two-phase system with a phase transfer catalyst, under conditions similar to those used in the synthesis of $(H_3Si)_4C$.[14] The key to the successful synthesis of **4** is the extremely low vapor pressure of squalene, which provides a very effective separation of the compound from the solvent. Other more common high-boiling solvents, including tetrahydronaphthalene and triglyme, did not completely separate from $(H_3Ge)_4C$, and, consequently, we obtained either contaminated products or extremely low yields of the pure compounds.

Compounds **4** (a waxy solid) and **3** (a liquid) are colorless low-volatility species (2 and 20 Torr at 22 °C, respectively) and are readily identified and characterized by their infrared (IR), NMR, and mass spectra (see Experimental Section). The reduction of **1** with $LiAlH_4$, under conditions similar to those for the reduction of **2**, leads to compounds **3** and **4** in 1:1 molar ratio in approximately 12% yield each. Incomplete reduction led to the formation of a $CGe_4H_4(H_xCl_{8-x})$ ($x = 0-8$) species that were isolated as colorless liquids and were identified by IR, NMR, and mass spectrometry. Various impurity levels of partially reduced tetragermyl methanes were consistently found in the reduction of **1** by $LiAlH_4$. This indicates that the strong

---

[8] Kouvetakis, J.; Chandrasekhar, D.; Smith, D. J. *Appl. Phys. Lett.* **1998**, *72*, 930.

[9] Rucker, H.; Methfessel, M.; Bugiel, E.; Osten, H. *J. Phys. Rev. Lett.* **1994**, *79*, 3578.

[10] Matsunaga, P. T.; Kouvetakis, J.; Groy, T. L. *Inorg. Chem.* **1995**, *34*, 5103−5104.

[11] Hoffman, L.; Bach, J. C.; Nielsen, B. B.; Jones, R.; Leary, P.; Oberg, S. *Phys. Rev. B* **1997**, 11167.

[12] For reviews of dihalogermylene chemistry see: (a) Rivière, P.; Rivière-Baudet, M.; Satgé, J. In *Comprehensive Organometallic Chemistry*; Wilkinson, G., Ed.; Pergamon: Oxford, 1982; Vol. 2, Chapter 10, p 399. (b) Satgé, J.; Massol, M.; Rivière, P. *J. Organomet. Chem.* **1973**, *56*, 1. (c) Margrave, J. L.; Sharp, K. G.; Wilson, P. W. *Fortschr. Chem. Forsch.* **1972**, *26*, 1. (d) Nefedov, O. M.; Manakov, M. N. *Angew. Chem., Int. Ed. Engl.* **1966**, *5*, 1021.

[13] (a) Kaczmarczyk, A.; Millard, M.; Nuss, J. W.; Urry, G. *J. Inorg. Nucl. Chem.* **1964**, *26*, 421. (b) Müller, R.; Müller, W. *Chem. Ber.* **1963**, *96*, 2894. (c) Köbrich, G.; von Nagel, R. *Tetrahedron Lett.* **1970**, 4693. (d) Gilman, H.; Smith, C. L. *J. Am. Chem. Soc.* **1964**, *86*, 1454. (e) Brook, A. G.; Abdesaken, F.; Söllradl, H. *J. Organomet. Chem.* **1986**, *299*, 9.

[14] (a) Schmidbaur, H.; Zech, J. *Eur. J. Solid State Inorg. Chem.* **1992**, *29*, 5. (b) Hager, R.; Steigelmann, O.; Müller, G.; Schmidbaur, H.; Robertson, H. E.; Rankin, D. W. H. *Angew. Chem., Int. Ed. Engl.* **1990**, *29*, 201.

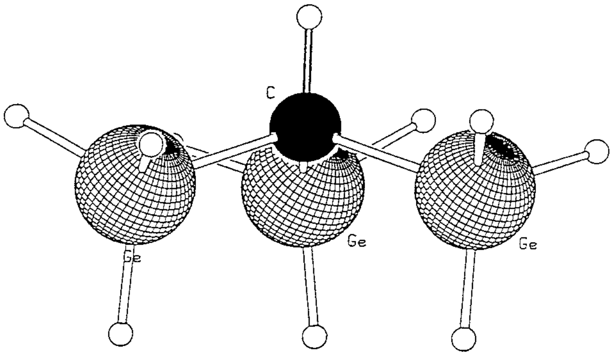

**Figure 1.** Molecular model of $(GeH_3)_3CH$ with $C_3$ symmetry and torsional angle $\tau(HCGeH) = 173°$. If the torsional angle $\tau(HCGeH) = 180°$ as indicated by the DFT calculations, the symmetry is $C_{3v}$.

Ge−Cl bonds in the molecule are much more difficult to reduce than the Ge−Br bonds and thus the overall yield of **4** obtained from the reduction **1** (12.5%) is substantially less than that obtained from the reduction **2** (20%). For this reason, $(Br_3Ge)_4C$ (**2**) is clearly a better precursor to $(GeH_3)_4C$ (**4**) than is $(Cl_2BrGe)_4C$ (**1**). $(GeH_3)_3CH$ (**3**) is also conveniently prepared via reduction of the corresponding tris(tribromogermyl)methane, $(GeBr_3)_3CH$ (**5**). The bromide in turn is prepared by direct insertion of $GeBr_2$ into the C−Br bonds of bromoform, $CHBr_3$ (eqs 3 and 4).

$$HCBr_3 + 3GeBr_2{\bullet}dioxane \rightarrow \underset{\mathbf{5}}{(Br_3Ge)_3CH} + 3dioxane \quad (3)$$

$$\underset{\mathbf{5}}{4(Br_3Ge)_3CH} + 9LiAlH_4 \rightarrow \underset{\mathbf{4}}{4(GeH_3)_3CH} + 9LiBr + 9AlBr_3 \quad (4)$$

Compound **5** is a colorless, air-sensitive solid, and its identity has been established by FTIR, NMR, GCMS, and elemental analysis. Its reduction with $LiAlH_4$ in dibutyl ether produces **3** in 20% yield.

**Structures of $(H_3Ge)_4C$ (4) and $(H_3Ge)_3CH$ (3) as Determined by Electron Diffraction and Density Functional Theory Calculations.** The gas-phase molecular structures of **3** and **4** have been determined by electron diffraction (GED) and density functional theory (DFT) calculations. The structure refinement of **3** was based on a model of $C_3$ symmetry characterized by six structural parameters: the Ge−C, Ge−H, and C−H bond lengths, the <GeCGe and <GeCH bond angles, and the torsional angle $\tau(H^*CGeH)$ (Figure 1). Values of the parameters derived from the GED data are presented in Table 1. The Ge−C bond distance in **3**, 1.960 (4) Å, is 0.010−0.015 Å longer than that in known carbogermanes, as illustrated in the following examples: $r(Ge-C) = 1.945$ Å in $Ge(CH_3)_4$,[15a] 1.947 Å in $GeH(CH_3)_3$,[15b] 1.950 Å in $GeH_2(CH_3)_2$,[15c] and 1.945 Å in $GeH_3CH_3$.[15d] The difference is at the edge of statistical significance. If real, the observed bond elongation and the small, but statistically significant widening of the <GeCGe angle [111.6 (2)°] relative to the tetrahedral value may be due to the steric repulsions between the germyl groups. Both differences are small, however, and they indicate that the $(H_3Ge)_3CH$ molecule is relatively free of strain. The best value obtained for the dihedral angle, $\tau(H^*CGeH) = 173(25)°$, is not significantly different from that corresponding to a staggered orientation of the germyl groups (180°). The huge estimated standard deviation of $\tau$ shows that the GED data contain very little information about the orientation of the germyl groups. Density functional calculations reproduce the observed Ge−C and Ge−H distances to better than 0.03° (Table 1) with good agreement between theory and experiment. Experimental and calculated molecular intensity curves are compared in Figure 2 and calculated radial distribution curves are shown in Figure 3.

**Table 1.** Interatomic Distances ($r$), Root Mean Square Vibrational Amplitudes ($l$), and Thermal Correction Terms ($D$) in Å and Valence and Torsional Angles in deg for $(GeH_3)_3CH$ (**3**) Obtained by Gas Electron Diffraction (GED) and (DFT) Calculations[c]

| | DFT | | | GED | |
|---|---|---|---|---|---|
| | $r$ | $l$ | $D$ | $r$ | $l$ |
| Bond Distances | | | | | |
| Ge−C | 1.936 | 0.051 | −0.004 | 1.960 (4) | 0.061 (2) |
| Ge−H | 1.535 | 0.091 | −0.079 | 1.535 (4) | 0.118 (4) |
| C−H*[a] | 1.095 | 0.079 | −0.012 | 1.070 (3) | [0.079] |
| Nonbonded Distances | | | | | |
| Ge···Ge | 3.164 | 0.108 | 0.002 | 3.234 (3) | 0.119 (2) |
| Ge···H* | 2.522 | 0.125 | −0.003 | 2.490 (2) | 0.170 (3) |
| Ge···H | 3.550 | 0.299 | −0.005 | 3.570 (30) | 0.250 (5)[b] |
| Ge···H | 4.526 | 0.127 | −0.024 | 4.500 (2) | 0.160 (2) |
| Ge···H | 3.497 | 0.284 | −0.060 | 3.500 (26) | 0.240 (5)[b] |
| C···H | | 0.135 | | 2.820(2) | [0.135] |
| Valence Angles | | | | | |
| <GeCH | 109.4 | | | 107.2 (2) | |
| <GeCGe | 109.5 | | | 111.6 (2) | |
| <CGeH | 109.5 | | | 108.0 (14) | |
| $\tau$(HCGeH) | 180.0 | | | 173.0 (25) | |
| $R$-factor | | | | 0.038 | |

[a] The unique H atom is designated by H*. [b] These amplitudes were refined with constant difference. [c] Nonrefined parameters in square brackets. Estimated standard deviations in parentheses in units of the last digit.

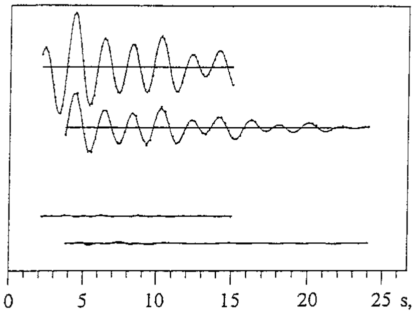

**Figure 2.** Top: Modified experimental (dots) and calculated (full lines) molecular intensity curves for $(GeH_3)_3CH$. Bottom: difference curves.

DFT structure optimization of **4** under $T$ symmetry yielded the parameters listed in Table 2. Note that the dihedral angle $\tau(GeCGeH)$ optimized to 180° corresponds to a configuration of staggered germyl groups and $T_d$ molecular symmetry. Structure refinements of the GED data were nevertheless carried out with a model of $T$ symmetry (Figure 4). The best value obtained for the dihedral angle was 162(2)°. If the estimated standard deviation is taken at its face value, this result indicates that the equilibrium structure of the molecule is one where the germyl groups have been rotated 18(2)° away from the staggered orientation (the corresponding rotation for the $C(SiH_3)_4$ compound is 20.04°[14b]). It is, however, possible that the deviation is an artifact due to inadequate treatment of the large amplitude torsional motion of the $GeH_3$ groups: DFT structure optimization of a model of $T$ symmetry in which the four germyl groups are rotated away from the staggered rotation yield an energy of

---

(15) (a) Hencher, J. L.; Mustoe, F. J. *Can. J. Chem.* **1975**, *53*, 3542. (b) Durig, J. R.; Chen, M. M.; Li, Y. S.; Turner, J. B. *J. Phys. Chem.* **1977**, *77*, 227. (c) Thomas, E. C.; Laurie, V. W. *J. Chem. Phys.* **1969**, *50*, 3512. (d) Laurie, V. W. *J. Chem. Phys.* **1959**, *30*, 1210.

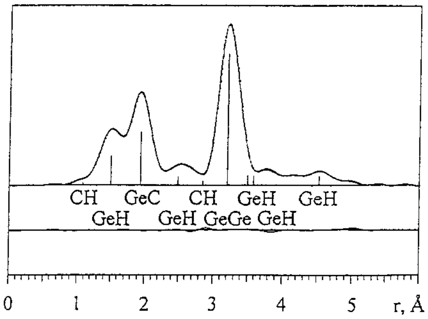

**Figure 3.** Top: experimental (dots) and calculated (full lines) radial distribution curves for (GeH$_3$)$_3$CH. Major interatomic distances are indicated by bars of height approximately proportional to the area under the corresponding peak. Bottom: difference curves. Artificial damping constant: 0.0025 Å.

**Table 2.** Interatomic Distances (*r*), Root Mean Square Vibrational Amplitudes (*l*), and Thermal Correction Terms (*D*) in Å and Valence and Torsional Angles in deg for (GeH$_3$)$_3$C (**4**) Obtained by Gas Electron Diffraction (GED) and (DFT) Calculations[b]

| | DFT | | | GED | |
|---|---|---|---|---|---|
| | *r* | *l* | *D* | *r* | *l* |
| | Bond Distances | | | | |
| Ge−C | 1.931 | 0.050 | −0.005 | 1.970 (2) | 0.055 (4) |
| Ge−H | 1.538 | 0.087 | −0.040 | 1.532 (5) | 0.094 (6) |
| | Nonbonded Distances | | | | |
| Ge···Ge | 3.154 | 0.115 | 0.001 | 3.207 (4) | 0.102 (2) |
| Ge···H | 3.532 | 0.254 | 0.000 | 3.500 (2) | 0.112 (2) |
| Ge···H | 3.530 | 0.254 | 0.000 | 3.870 (3) | 0.210 (3) |
| Ge···H | 4.509 | 0.127 | −0.014 | 4.560 (13) | 0.180 (2) |
| C···H | 2.856 | 0.134 | −0.02.4 | 2.970 (2) | [0.134] |
| | Valence Angles | | | | |
| <Ge−C−Ge | [109.5] | | | [109.5] | |
| <Ge−C−H | 110.5 | | | 116.0 (2) | |
| τ(GeCGeH) | 180.0 | | | 162.0 (2) | |
| *R*-factor[a] | | | | 0.035 | |

[a] $R = \sqrt{[\sum w(I_{\text{obs}} - I_{\text{calc}})^2 / \sum w(I_{\text{obs}})^2]}$. [b] Nonrefined parameters in square brackets. Estimated standard deviations in parentheses in units of the last digit.

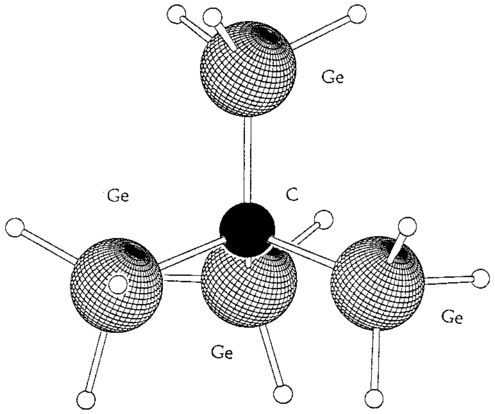

**Figure 4.** Molecular model of (H$_3$Ge)$_4$C with *T* symmetry and torsional angle τ(GeCGeH) = 162°. If τ(GeCGeH) = 180° as indicated by the DFT calculations, the symmetry is $T_d$.

7.0 kJ mol$^{-1}$ above the staggered equilibrium structure, while the thermal energy associated with the vibration of the four groups at room temperature is 10 kJ mol$^{-1}$. Experimental and calculated molecular intensity curves for **4** are compared in Figure 5, and calculated radial distribution curves are shown in Figure 6.

The Ge−C bond distance in **4**, 1.970(2) Å, is significantly longer than the Ge−C bond lengths listed above. The difference is, however, small only 0.02 Å and indicates that **4** like **3** [Ge−C = 1.960 (4) Å] is relatively free of strain. This is in strong contrast with the Ge−C bond length obtained from the gas-phase structure of (Br$_3$Ge)$_4$C (**2**),[16] [2.042(8) Å], which is about 0.10 Å longer than that in the previously described methylgermanes. We suggest that the Ge−C elongation observed in **2** is due primarily to Br···Br repulsions and to a lesser extent to Ge···Ge and Ge···Br repulsions. The Ge−Br bond distance in (Br$_3$Ge)$_4$C (**2**) [2.283(3) Å] is nevertheless normal based on a comparison with the bond distances in GeH$_2$Br$_2$ [2.277(3) Å][17a] and GeBr$_4$ [2.272(3) Å].[17b]

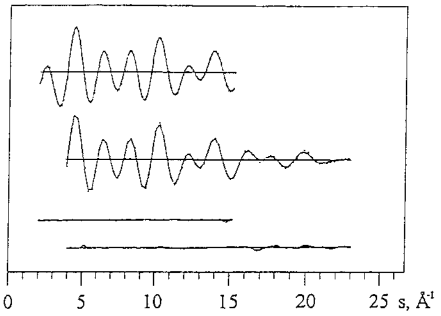

**Figure 5.** Top: modified experimental (dots) and calculated (full line) molecular intensity curves for (H$_3$Ge)$_4$C. Bottom: difference curves.

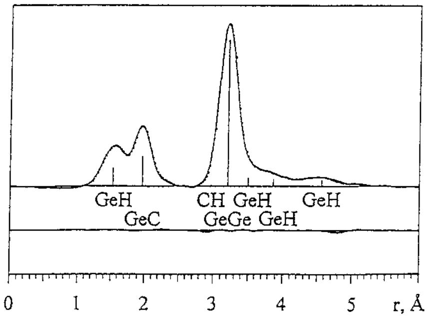

**Figure 6.** Top: experimental (dots) and calculated (full lines) radial distribution curves for (H$_3$Ge)$_4$C. Major interatomic distances are indicated by bars of height approximately proportional to the area under the corresponding peak. Bottom: difference curve. Artificial damping constant: 0.0025 Å$^2$.

Steric nonbonded Ge−Ge repulsion arguments causing elongation of the Ge−C bond have been used to predict that the (H$_3$Ge)$_4$C (**4**) molecule is unstable.[18] Similarly, it was suggested that the analogous Si compound, (H$_3$Si)$_4$C, would be very difficult to prepare. Nevertheless, both compounds are readily obtained and display rather normal Si−C (1.875 Å)[14b] and Ge−C (1.97 Å) bond lengths as shown by gas-phase electron diffraction studies.

Finally we comment on the relevance of this study on structural characterizations of substitutional carbon in Ge crystals. Since substitutional carbon in Si has been known for decades, the similarities between Si and Ge suggest that substitutional carbon should also exist in Ge. Moreover, the higher bond dissociation energy of Ge−C (4.7 eV) compared to that of Ge−Ge (2.8 eV) supports the existence of subtitutional Ge$_{1-x}$C$_x$.[19] The fact that the solubility of carbon in Ge is

---

[16] Haaland, A.; Shorokhov, D. J.; Strand, T. G.; Kouvetakis, J.; O'Keeffe, M. *Inorg. Chem.* **1997**, *36*(23), 5198.

[17] (a) Beagley, B.; Brown, D. P.; Freeman, J. M. *J. Mol. Struct.* **1973**, *18*, 335. (b) Souza, G. C. B.; Wieser, J. D. *J. Mol. Struct.* **1975**, *24*, 442.

[18] Toman, J. J.; Frost, A. A.; Topiol, S.; Jacobson, S.; Ratner, M. *Theor. Chim. Acta* **1981**, *58*, 285.

[19] Gaydon, A. G. *Dissociation of Energies and Spectra of Diatomic Molecules*, 3rd ed.; Chapman and Hall: London, 1968.

extremely low ($10^{8}-10^{10}$ cm$^{-3}$)[20] compared to the solubility of carbon in Si ($3.5 \times 10^{17}$ cm$^{-3}$) indicates that strain due to the large difference between the Ge−C (1.94 Å) and Ge−Ge (2.40 Å) may make the formation of substitutional $Ge_{1-x}C_x$ unfavorable. The present work demonstrates that there is very little strain associated with an isolated $Ge_4C$ tetrahedral cluster terminated by hydrogens, whereas substantial strain seems to exist in the analogous $Ge_4C$ cluster terminated by Br atoms as in compound **2**. The strain in the latter is relieved, however, by a marked elongation of the Ge−C bond and rotation of the terminal $-(Br)_3$ groups away from $T_d$ symmetry to minimize repulsions (Figure 7). Nevertheless, compound **2** remains remarkably stable indicating that unusually long Ge−C bonds can exist without fragmenting. Thus the formation of $Ge_{1-x}C_x$ alloys which require stretched Ge−C bonds may be possible under metastable conditions. The existence of stretched Ge−C bonds is consistent with recent theoretical modeling of carbon sites in extended $Ge_{1-x}C_x$ lattices and with higher than expected (by Vegard's law) lattice constants in Ge−C heterostructures grown by CVD, as detailed below.

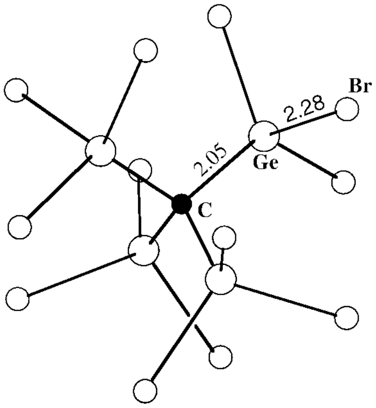

**Figure 7.** A representation of $(Br_3Ge)_4C$ with *T* symmetry. The Ge−C bond is 0.10 Å longer than in typical carbogermanes, and the arrangement of the Br atoms is close to icosahedral to minimize strain. The Ge−Br bond distance compared to those of $GeBr_4$ and $GeH_2Br_2$ appears to be normal.

**Growth of $Ge_4C$ and $Si_x(Ge_4C)_y$ Materials Using $C(GeH_3)_4$ (4).** We explored the thermal decomposition of $C(GeH_3)_4$ on chemically clean (100)Si surfaces in our UHV−CVD reactor at 500 °C using ultrahigh purity $H_2$ as the carrier gas. The decomposition under these conditions produced a light brown thin film material which has Ge and C in the ratio of approximately 4:1 and a thickness of 1000 Å. The composition was established by Rutherford backscattering spectroscopy (RBS) (utilizing a carbon resonance reaction) and corresponds to the same atomic ratio as in the precursor, suggesting that the $Ge_4C$ composition and possibly the tetrahedral arrangement of the gaseous molecule is retained in the deposited film. The decomposition reaction of $C(GeH_3)_4$ occurs via loss of $H_2$, while the $Ge_4C$ core is maintained intact as illustrated in eq 5. This is consistent with the decomposition of the molecule in the mass spectrometer. The mass spectrum of $C(GeH_3)_4$ shows an isotopic pattern centered at 308 amu corresponding to $CGe_4H_x$ suggesting that although the molecule appears to lose $H_2$ in the mass spectrometer, the $Ge_4C$ core is retained in the gas phase.

$$C(GeH_3)_4 \rightarrow Ge_4C + 6H_2 \qquad (5)$$

High-resolution transmission electron microscopy (TEM) observations from cross-sectional samples and atomic force microscopy (AFM) studies revealed islandlike growth of completely crystalline but also defective material. Analysis of the TEM micrographs indicated that the material had the diamond cubic structure and that the average lattice constant was slightly lower than that of Ge and was substantially higher than the value calculated by Vegard's law. These calculations assume linear interpolation between the unit cell parameters of C (diamond) and pure Ge and that the Ge−C bond length in the material will have the "normal" value of 1.94 Å as detailed earlier. On the other hand, the Ge−C bond can stretch substantially in a highly strained environment, and we have demonstrated significantly higher than normal experimental bond lengths in the sterically crowded model compound $C(GeBr_3)_4$ (**2**). In addition, theoretical investigations recently revealed that the Ge−C bonds at random substitutional sites of C in Ge must be stretched to accommodate strain, and a typical bond length is reported to be 2.046 A.[19] This is in remarkable agreement with the experimental value we determined for $C(GeBr_3)_4$ by gas-phase electron diffraction (2.05 Å) and single-crystal X-ray structure determination (2.05 Å). Furthermore, theoretical studies of the Si analogue ($Si_4C$) have shown that the C−Si bond is stretched by at least 7% relative to the $\beta$-SiC to accommodate strain.[9] We should note that the electron micrographs do not show any amorphous or crystalline carbon precipitation, indicating that the majority of the carbon concentration should be part of the lattice. Electron energy loss spectroscopy (EELS) suggests that the carbon is diamond-like ($sp^3$ hybridized) as expected for a $Ge_4C$ tetrahedral structure and confirms the absence of graphitic carbon. Precipitation of GeC, analogous to SiC, is doubtful since this compound is predicted to be metastable with respect to its elements, and it has not yet been prepared as a crystalline phase. We cannot rule out, however, that the extensive defects might represent ordering of the elements in the cubic lattice with the carbon occupying a common sublattice to relieve strain. Clearly, at this stage, material with better crystallinity is needed to determine accurately the lattice constant of the $Ge_4C$ composition by TEM and high-resolution X-ray diffraction, and, hopefully, we will then be able to understand the effect of carbon concentration in the lattice parameter of this intriguing material.

The utility of $C(GeH_3)_4$ as a carbon source for growth of high quality-epitaxial $Ge_{1-x}C_x$ layers on Si and $Ge_{1-x}C_x$ quantum structures (dots) on $Ge_{1-x}C_x$/Si was also demonstrated. In addition, a reaction of $C(GeH_3)_4$ with disilane ($H_3Si-SiH_3$) at 475 °C on a chemically pure (native oxide free) Si substrate followed by annealing at 750 °C of the deposited film yielded a random SiGeC alloy material with composition $Si_{75}Ge_{20}C_5$. This composition, as determined by RBS, clearly shows that the germanium and carbon in the film are in the same ratio (4:1) as in the gaseous precursor, suggesting that the molecule has retained its compositional integrity during growth. TEM examinations revealed that the entire layer of $Si_{75}Ge_{20}C_5$ was crystalline and heteroepitaxial. A typical electron micrograph demonstrating the heteroepitaxial character of the material is illustrated in Figure 8. Optical diffractogram analysis of the crystal lattice fringes revealed an average lattice parameter that is very close to that of Si. Ion channeling experiments confirmed that the material is epitaxial and of high crystal quality.

Our preliminary deposition results indicate that $C(GeH_3)_4$ is a very promising carbon source for the development of metastable $Si_{1-x-y}Ge_xC_y$ phases that contain substantial amounts of carbon. It offers significant improvements to other SiGeC precursors in allowing compositional control and low deposition

---

(20) Scace, R. I.; Slack, G. A. *J. Chem. Phys.* **1959**, *30*, 1551.

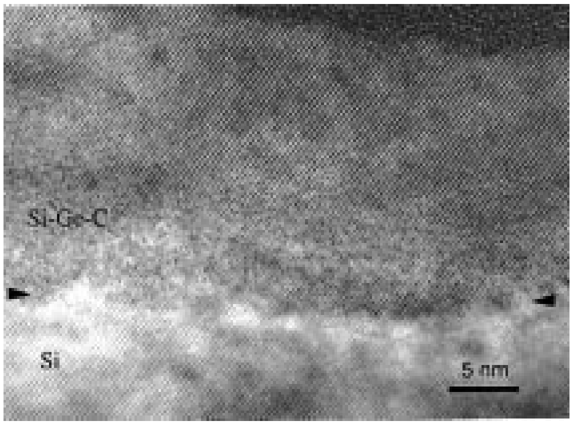

**Figure 8.** Cross-sectional electron micrograph demonstrating the heteroepitaxial growth of $Si_{75}Ge_{20}C_5$ obtained from reactions using $(H_3Ge)_4C$ as the carbon source. The [111] lattice fringes (*d* spacing of approximately 3.136 Å) of the diamond cubic structure are visible and indicate relatively defect-free Si/SiGeC interface.

temperature because it lacks strong C−H bonds, and it incorporates a tetrahedral core that is structurally consistent with the silicon substrate. In addition, the encapsulation of carbon between four Ge centers should prevent Si−C bond formation that might eventually lead to silicon carbide (SiC) precipitation.

## Conclusion

We have used germylene insertion chemistry to construct extremely stable (despite the large amount of steric bulk) trihalogermyl methanes containing a central carbon tetrahedrally encapsulated within a germanium environment. Their reduction with $LiAlH_4$ leads to the formation of trigermyl- $(H_3Ge)_4C$ and tetragermylmethane $(H_3Ge)_3CH$, crucial precursors for UHV−CVD growth of new group IV compounds and alloys that incorporate $Ge_4C$ building blocks. These diamond-structured materials may have applications in microelectronics for silicon based band gap engineering and lattice matching. The $(H_3Ge)_4C$ compound in particular provides a unique, and potentially practical, low-temperature route for development of Ge based semiconductor materials on single-crystal Si via heteroepitaxial methods. The islandlike 3-D nucleation that occurs during growth (Stranski-Krastanov mode), and the high defect density observed at the Si-epilayer interface which is detrimental to device performance, has been suppressed by the incorporation of carbon. The smaller size of C compensates for the larger size of Ge in the crystal.

## Experimental Section

**General Considerations.** Reactions were performed under prepurified nitrogen using standard Schlenk and drybox techniques. Dry, air-free solvents were distilled from sodium benzophenone ketyl prior to use. $^1H$ (300 MHz) and $^{13}C$ (125.7 MHz) NMR spectra were recorded on a Varian Gemini 300 and a Varian Unity 500 spectrometer, respectively, and were referenced to the solvent resonances ($C_6D_6$, $^1H$: $\delta$ 7.15; $^{13}C$: $\delta$ 128.0). FTIR spectra were recorded on a Nicolet Magna-IR 550 spectrometer either as a Nujol mull between KBr plates or in a 10 cm gas cell with KBr windows. Elemental analyses were performed by Desert Analytics (Tucson, AZ). Electron impact mass spectra were performed on a Finnigan-MAT Model 312 mass spectrometer (IE = 70 eV, Source $T$ = 225 °C) in the ASU departmental mass spectrometry facility or at the Midwest Center for Mass Spectrometry (Lincoln, NE). Carbon tetrabromide (Aldrich) and benzyltriethylammonium chloride (Aldrich) were used as received. Lithium aluminum hydride (Aldrich) was recrystallized from diethyl ether prior to use. Germanium tetrachloride was purchased from Aldrich and used without further purification. Germanium tetrabromide was synthesized from the elements. Triethylsilane (Aldrich) was refluxed over 4 Å molecular sieves for 4 h and then distilled at 105 °C and 760 Torr. The *p*-dioxane (Aldrich) was dried over sodium benzophenone ketyl and freshly distilled before use. We synthesized $GeX_2$·dioxane (X = Cl, Br) using a method similar to that described by Herrmann et al. (European Patent 568074). We found, however, that the isolation of high purity material in high yield (over 70%) is principally dependent on the experimental conditions which have not yet been given in detail. Here we report a detailed procedure to synthesize pure complexes in yields greater than 70%. Uncontaminated $GeCl_2$·dioxane and $GeBr_2$·dioxane starting materials are absolutely necessary for the successful synthesis of the $(BrCl_2Ge)_4C$ and $(BrCl_2Ge)_4C$ as described below.

**$GeCl_2$·dioxane.** A 500 mL flask was charged with $GeCl_4$ (15.0 g, 0.070 mol), $(C_2H_5)_3SiH$ (16.38 g, 0.140 mol), *p*-dioxane (42.0 g, 0.477 mol), toluene (100 mL), and $LiAlH_4$ (100 mg). The mixture was heated under nitrogen at 85−86 °C for 14 h with continuous stirring. The temperature was then increased to 100 °C, and the solution was then monitored carefully for color change. After 4 h, the color of the solution changed sharply from light yellow to a rusty orange. At this point, the heating was stopped immediately, and the solution was filtered hot in the inert atmosphere box. Care was taken not to contaminate the solution with any of the red insoluble material that settled on the bottom of the flask. The insoluble solid was washed several times with hot toluene, and the combined clear filtrates were cooled at −23 °C to yield transparent needlelike crystals. Concentration and cooling of the solution produced several crops of these crystals to give an overall yield of 70%. The product was characterized by IR and NMR. IR (Nujol): 1294 (s), 1258 (s), 1114 (s), 1078 (s), 902 (s), 747−725 (w, br), 628 (s), 499 (m). $^1H$ NMR ($CDCl_3$): $\delta$ 3.25 (s).

**$GeBr_2$·dioxane.** A 500 mL flask was charged with $GeBr_4$ (20.0 g, 0.051 mol), $(C_2H_5)_3SiH$ (13.0 g, 0.111 mol), *p*-dioxane (32.0 g, 0.363 mol), toluene (100 mL), and $LiAlH_4$ (100 mg). The solution was initially stirred for 14 h at room temperature and then for approximately 6 h at 95 °C during which time it was carefully monitored for any significant color change. During the 6 h the solution changed color from yellow to clear and back to yellow and then finally turned orange. At this point, the solution was filtered hot, and the product was crystallized and isolated as colorless crystals (75% yield) using the same method described above for the chloride analogue. The IR and NMR spectra of the product were recorded. The main impurity was found to be $GeBr_4$·dioxane which was identified by its IR and mass spectra. The mixture was extracted several times with cold toluene to separate the soluble $GeBr_4$·dioxane from the relatively insoluble $GeBr_2$·dioxane. IR (Nujol): 1334 (w), 1299 (w), 1284 (s), 1251(s), 1102 (vs), 1073 (vs), 1035 (s), 1013 (w), 892 (s), 840 (vs), 753−725 (w, br), 621 (vs), 285 (vs). $^1H$ NMR ($CDCl_3$): $\delta$ 3.25 (s).

**Preparation of $(BrCl_2Ge)_4C$ (1).** A solution of $CBr_4$ (0.72 g, 2.2 mmol) in toluene (10 mL) was added to a suspension of $GeCl_2$·dioxane (2.00 g, 8.64 mmol) in toluene (50 mL). The mixture was stirred at ambient temperature for 2 h during which time most of the solid dissolved. The mixture was then heated to 80 °C for 1 h and filtered hot. Concentration and cooling of the resulting colorless solution produced several crops of blocky, colorless crystals in a total yield of 1.56 g (1.72 mmol, 79%). Mp 330 °C (dec). IR (Nujol): 701 (vs, GeC str), 447 (vs, GeCl str), 421 (s, GeCl str), 407 (m, sh, GeCl str), 336 (m, GeBr str), 315 (m, GeBr str), 305 (m, sh, GeBr str). EIMS (*m*/*e*): Shows halide scrambling with isotopic envelopes centered at 1004 ($CBr_7Cl_4Ge_4^+$), 958 ($CBr_6Cl_5Ge_4^+$), 914 ($CBr_5Cl_6Ge_4^+$), 870 ($CBr_4Cl_7Ge_4^+$), 826 ($CBr_3Cl_8Ge_4^+$), 782 ($CBr_2Cl_9Ge_4^+$), 736 ($CBrCl_{10}Ge_4^+$), 692 ($CCl_{11}Ge_4^+$). Anal. Calcd for $CBr_4Cl_8Ge_4$: C, 1.33; Br, 35.3; Cl, 31.3. Found: C, 1.57; Br, 33.3; Cl, 32.8.

**Preparation of $(Br_3Ge)_4C$ (2).** Compound **2** was synthesized analogously to **1** from $CBr_4$ (1.29 g, 3.89 mmol) and $GeBr_2$·dioxane (5.00 g, 15.6 mmol). The yield of colorless **2** was 4.60 g (3.65 mmol, 94%). Mp 329 °C (dec). IR (Nujol): 672 (vs, GeC str), 330 (vs, GeBr str). EIMS (*m*/*e*): 1261 ($M^+$), 1182 ($M^+ - Br$), 870 ($M^+ - GeBr_4$). Anal. Calcd for $CBr_{12}Ge_4$: C, 0.95; Br, 76.0. Found: C, 1.09; Br, 75.8.

**Preparation of $(H_3Ge)_3CH$ (3) and $(H_3Ge)_4C$ (4) by Reduction of 2 with $LiAlH_4$.** A flask was charged with **2** (3.00 g, 2.36 mmol), $LiAlH_4$ (0.542 g, 14.2 mmol), benzyltriethylammonium chloride (72 mg, 0.32 mmol), and squalene (45 mL). The mixture was stirred at ambient temperature for 3 days, then warmed to 60 °C, and stirred for an additional 6 h. The temperature was raised to 70−80 °C, and the mixture was evacuated for 8 h by dynamic vacuum through a trap held at −196 °C to collect the volatiles. The volatiles were then passed through traps held at −45, −78, and −196 °C. The bulk of the material from the −45 °C trap was $(H_3Ge)_4C$ **4**, but some $(H_3Ge)_3CH$ (**3**) was also obtained. The contents of the −78 °C trap were primarily $(H_3Ge)_3CH$ and a minor quantity of $(H_3Ge)_4C$ as indicated by NMR and IR. The −196 °C trap contained traces of germane, digermane, and another unidentified Ge hydride. Successive trap-to-trap distillations from −45 to −78 °C yielded fairly pure **4** (0.140 g, 0.445 mmol, ca. 20%). The combined fractions from the −78 °C trap gave **3** (0.110 g, 0.437 mmol, ca. 18%) with a trace of **4**. For **4**: Vapor pressure: ca. 1−2 Torr, 20 °C. IR (gas phase): 2075 (vs, GeH str), 888 (w, $GeH_3$ asym def), 839 (m, $GeH_3$ sym def), 793 (vs, GeC str), 745 (w), 704 (vw). $^1H$ NMR: $\delta$ 4.07 (s, Ge*$H_3$*). $^{13}C$ NMR: $\delta$ −37.09. EIMS (*m*/*e*): 298−316 ($CH_xGe_4^+$). For **3**: Vapor pressure: 20 Torr, 20 °C. IR (gas phase): 3032 (vw, CH str), 2075 (vs, GeH str), 1031 (vw, CH wag), 880 (w, $GeH_3$ asym def), 837 (m, $GeH_3$ sym def), 793 (w), 745 (s, GeC str), 704 (w). $^1H$ NMR: $\delta$ −0.60 (dect, C*H*), (coupling constant 3.9 Hz) 3.83 (d, Ge*$H_3$*). $^{13}C$ NMR: $\delta$ −28.46. EIMS (*m*/*e*): 222−244 ($CH_xGe_3^+$).

**Synthesis of $(H_3Ge)_3CH$ (3) and $(H_3Ge)_4C$ (4) by Reduction of 1 with $LiAlH_4$.** A flask was charged with **1** (1.5 g, 1.66 mmol), $LiAlH_4$ (0.30 g, 7.9 mmol), benzyltriethylammonium chloride (72 mg, 0.32 mmol), and squalene (25 mL). The mixture was stirred at ambient temperature for 3 days and at 60 °C for an additional 2 days. The mixture was evacuated for 8 h by dynamic vacuum through a trap held at −196 °C to collect the volatiles. The volatiles were then separated as described above to give **3** and **4** in about 12% yield each.

**Synthesis of $(Br_3Ge)_3CH$ (5).** Neat tribromomethane (0.525 g, 2.08 mmol) was added to a suspension of $GeBr_2$·dioxane (2.05 g, 6.40 mmol) in toluene (60 mL). The mixture was stirred at 85 °C for 3 days during which time most of the solid dissolved. The mixture was then filtered while hot. Concentration and cooling of the resulting solution produced several crops of a colorless solid in a total yield of 1.77 g (1.86 mmol, 89%). Mp 148−150 °C. IR (Nujol): 1016 (m, CH bend), 684 (vs, GeC str), 509 (s, GeC bend), 334 (vs, GeBr str). EIMS (*m*/*e*): shows isotopic envelopes centered at 870 ($Br_8Ge_3CH^+$), 638 ($Br_6Ge_2CH^+$), 557 ($Br_5Ge_2CH^+$), 478 ($Br_4Ge_2CH^+$), 395 ($Br_3Ge_2CH^+$), 325 ($Br_3GeCH^+$), 244 ($Br_2GeCH^+$), 233 ($Br_2Ge^+$) and 153 ($BrGe^+$). $^1H$ NMR: $\delta$ 3.54 (s, C*H*), $^{13}C$ NMR: $\delta$ 40.87 ppm. Anal. Calcd for $(Br_3Ge)_3CH$: Br, 75.7. Found Br, 75.5.

**Reduction of $(Br_3Ge)_3CH$ (5) with $LiAlH_4$.** A flask was charged with **5** (5.0 g, 5.26 mmol), benzyltriethylammonium chloride (0.25 g, 1.1 mmol), and $LiAlH_4$ (2.0 g, 52.7 mmol) in 1,2,3,4-tetrahydronaphthalene (THN) (60 mL). The mixture was stirred under nitrogen at ambient temperature for 3 days, followed by stirring at 60 °C for 5 h. The volatiles were then passed through traps held at −45, −78, and −196 °C. A very small quantity of $(GeH_3)_3CH$ and THN were collected at −45 °C, pure $(GeH_3)_3CH$ was collected at −78 °C, and a mixture of germane and methylgermane was collected at −196 °C. (14 L-Torr of **3**, 0.79 mmol, 15%).

**Structures of $HC(GeH_3)_3$ and $C(GeH_3)_4$: Experimental and Computational Data.** The molecular structures of **3** and **4** were optimized by density functional (DFT) calculations using the Gaussian 94 program system[21] with a standard 6-31G**(d,p) basis set and Becke's three-parameter hybrid method for exchange and exchange-correlation[22] with nonlocal correlation provided by the BW91 gradient-corrected functional.[23] Molecular force fields were calculated analytically. The DFT force fields were used to calculate root-mean-square vibrational amplitudes (*l*) and vibrational correction terms (*D*) at the temperatures of the gas electron diffraction experiments employing the ASYM40 program.[24] Molecular models (Figures 1 and 4) were drawn with the aid of the program PLUTON.[25]

Electron diffraction scattering data were recorded on the Balzers KDG2 system at Oslo[26] with the metal inlet system and sample reservoir at room temperature. Exposures were made with a nozzle to plate distance of about 50 and 25 cm. Structure refinements for **3** were based on data from six plates for each distance, and structure refinements for **4** were based on two plates exposed with the longer and six plates exposed with the shorter distance. The plates were scanned on an Agfa Arcus II scanner, and the data were processed as described elsewhere.[27] Atomic scattering factors were taken from ref 28. Backgrounds were drawn as least-squares adjusted polynomials to the difference between the total experimental and calculated molecular scattering intensities. The molecular structure refinements were carried out by least-squares calculations on modified molecular intensities using the program KCED 26 written by G. Gundersen, S. Samdal, H. M. Seip, and T. G. Strand.

The structure refinement of **3** was based on a molecular model of $C_3$ symmetry as indicated in Figure 1. The $CGeH_3$ fragments were assumed to have local $C_{3v}$ symmetry. The molecular structure is then determined by six independent structural parameters: the Ge−C, Ge−H, and C−H* bond distances; the valence angles <CGeH, and <GeCH; and a torsional angle $\tau$(H*CGeH). When $\tau = 180°$, the Ge−H bonds are staggered with respect to the Ge−C bonds originating from the C atom, and the molecular symmetry is $C_{3v}$. Least-squares refinements of the six structure parameters and six rms vibrational amplitudes yielded the best values listed in Table 1. Nonrefined vibrational amplitudes were fixed at calculated values. The *R* factors were calculated as $R[\sum(I_o - I_c)_2\sum I_o]^{1/2}$. For 25 cm data $R = 6.2\%$, for 50 cm data $R = 3.0\%$ and overall $R = 3.8\%$. Structure refinement of **4** was based on a model of *T* symmetry as shown in Figure 4. The molecular structure is determined by the Ge−C and Ge−H bond distances, the valence angle <CGeH, and a dihedral angle $\tau$(GeCGeH); when $\tau = 180°$ the Ge−H bonds, are staggered with respect to the Ge−C bonds and the molecular symmetry is $T_d$. Refinement of the four structure parameters and six vibrational amplitudes yielded the best values listed in Table 2. All refinements were carried out with diagonal weight matrixes, so the estimated standard deviations listed were doubled to include the added uncertainty due to data correlation as discussed by Seip et al.[29] and expanded to include a scale uncertainty of 0.1%.

**Acknowledgment.** The work at ASU was supported by a grant from the National Science Foundation (DMR-9458047). Partial support was provided by a grant from the Army Research Office (ARO) DAAH04-96-1-00229. We are grateful to the VISTA program of STATOIL and the Norwegian Academy of Science and Letters for financial support and to the Norwegian Research Council for a generous grant of computing time.

JA9810033

---

(21) Gaussian 94, revision D.2; Frisch, M. J.; Trucks, G. W.; Schlegel, H. B.; Gill, P. M. W. ; Johnson, B. G.; Robb, M. A.; Cheeseman, J. R.; Keith, T.; Peterson, G. A.; Montgomery, J. A.; Raghavachari, K.; Al-Laham, M. A.; Zakrzewski, V. G.; Ortiz, J. V.; Foresman, J. B.; Cioslowski, J. ; Stefanov, B. B.; Nanayakkara, A. Challacombe, M.; Peng, C. Y.; Ayala, P. Y.; Chen, W.; Wong, M. W.; Andres, J. L.; Repogle, E. S.; Gomperts, R.; Martin, R. L.; Fox, D. J.; Binkley, J. S.; Defrees, D. J.; Baker, J.; Stewart, J. P.; Head-Gordon, M.; Gonzales, C.; Pople, J. A. Gaussian, Inc.: Pittsburgh, PA, 1995.

(22) Becke, A. D. *J. Chem. Phys.* **1988**, *98*, 3098.

(23) Perdew, J. P.; Wang, Y. *Phys. Rev.* **1992**, *B45*, 13244.

(24) Hedberg. L.; Mills, I. M. *J. Mol. Spectrosc.* **1993**, *160*, 117.

(25) Spek, A. L. The Euclid Package. In *Computational Crystallography*; Sayre, D., Ed.; Clarendon: Oxford, 1982.

(26) Zeil, W.; Haase, J.; Wegmann, L. *Zeits. Instrumentk.* **1966**, *74*, 84.

(27) Gundersen, S.; Strand, T. G. *J. Appl. Cryst.* **1996**, *29*, 638.

(28) Ross, A. W.; Fink, M.; Hilderbrandt, R. *International Tables for X-ray Crystallography*; Wilson, A. J. D., Ed.; Kluwer Academic Publisher: Dodrecht, 1992; Vol. C, p 245.

(29) Seip, H. M.; Strand, T. G.; Stolevik, R. *Chem. Phys. Lett.* **1969**, *3*, 617.